Supplement of Ocean Sci., 20, 1–20, 2024
https://doi.org/10.5194/os-20-1-2024-supplement

Ocean Science
Open Access

Supplement of

Integration of microseism, wavemeter buoy, HF radar and hindcast data to analyze the Mediterranean cyclone Helios

Alfio Marco Borzì et al.

Correspondence to: Alfio Marco Borzì (alfio.borzi@phd.unict.it)

Supplementary figures

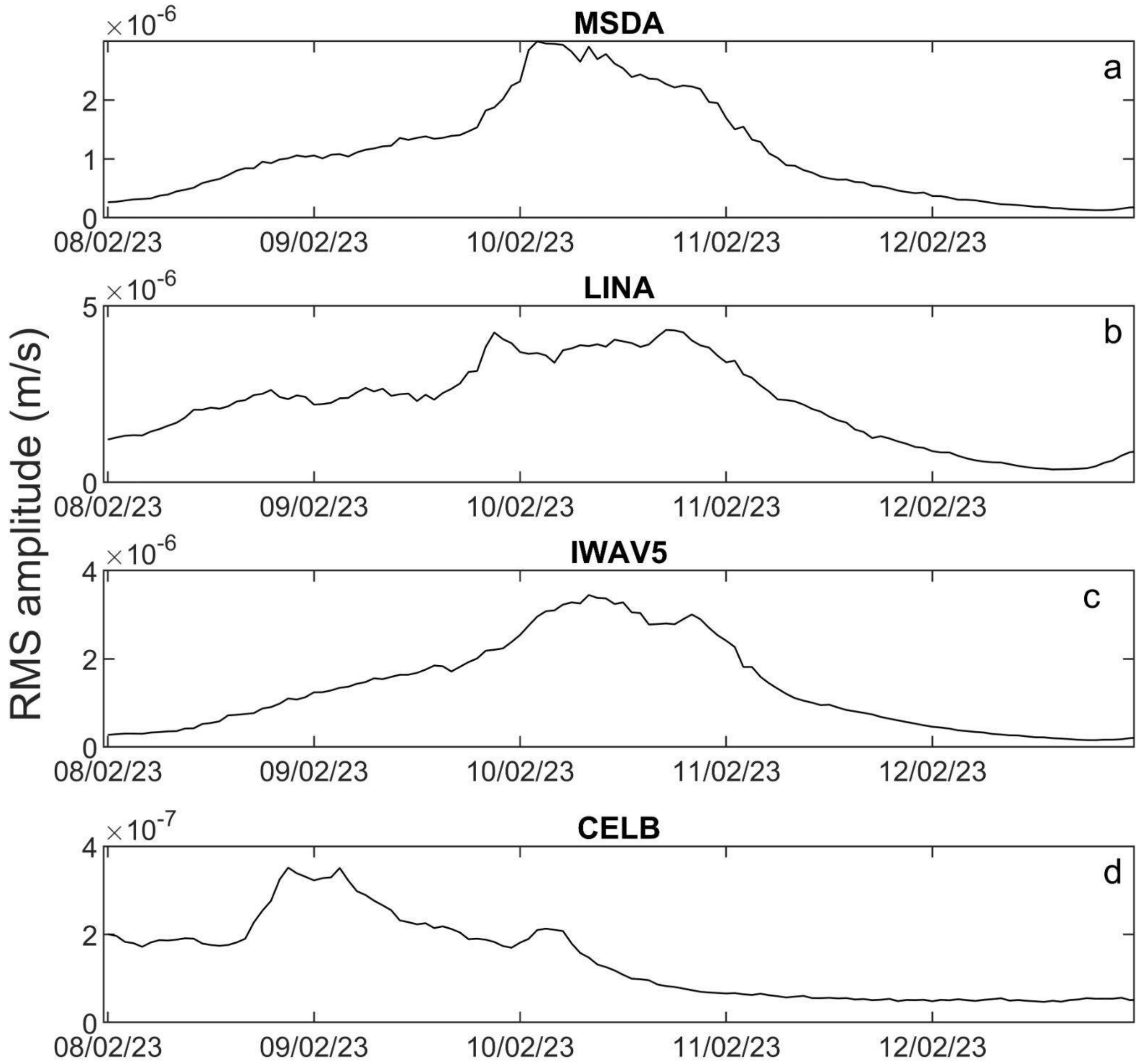

Figure S1: RMS amplitude time series, for the SPSM band (0.2-0.4 Hz), of the seismic signal recorded by the vertical component of 4 stations located along the Maltese coastline (a), in Linosa Island (b), in the southern part of Sicily (c) and in Central Italy (d) (see **Figure 2a** for the station locations).

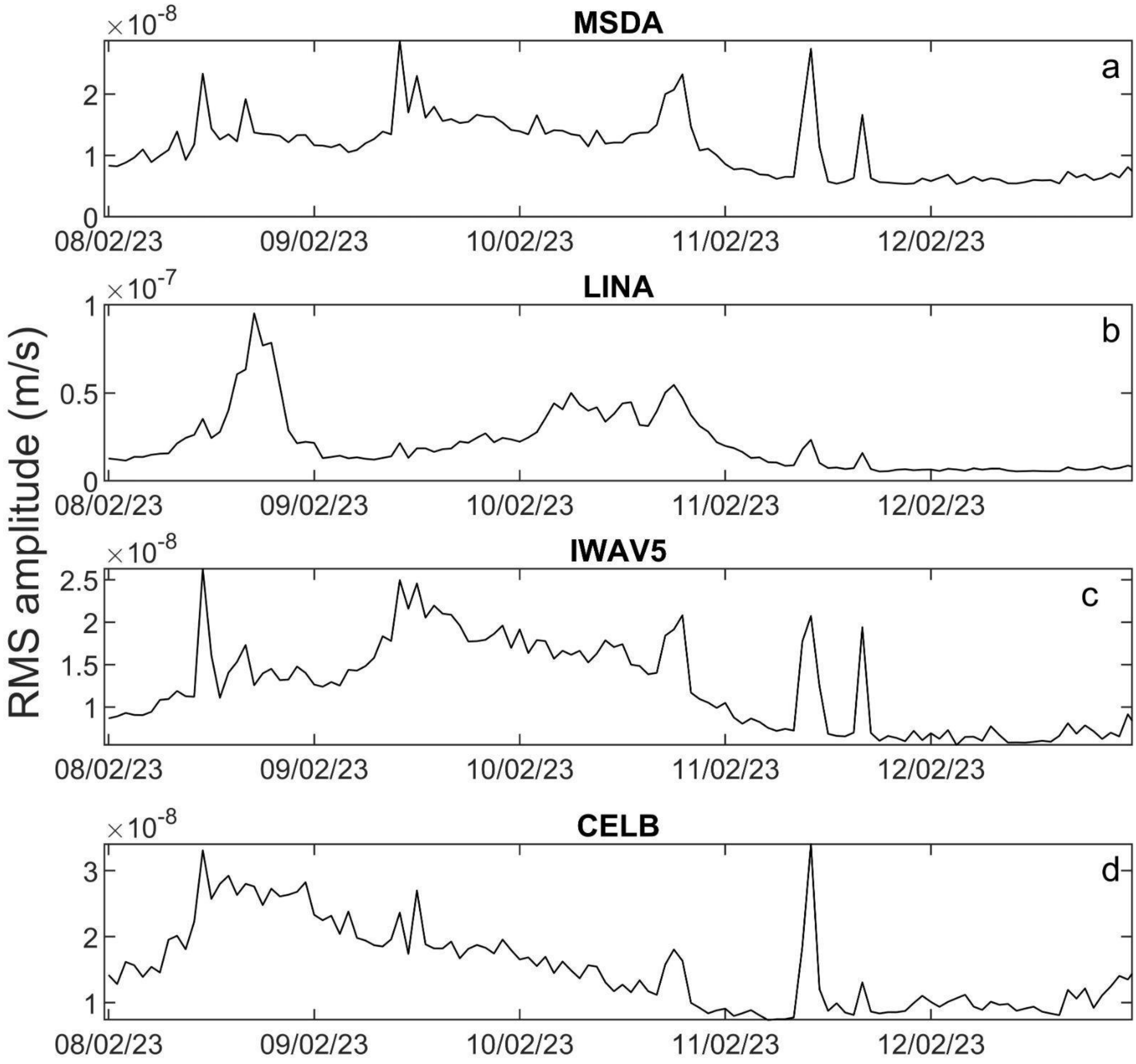

Figure S2: RMS amplitude time series, for the PM band (0.05-0.07 Hz), of the seismic signal recorded by the vertical component of 4 stations located along the Maltese coastline (a), in Linosa Island (b), in the southern part of Sicily (c) and in Central Italy (d) (see **Figure 2a** for the station locations).

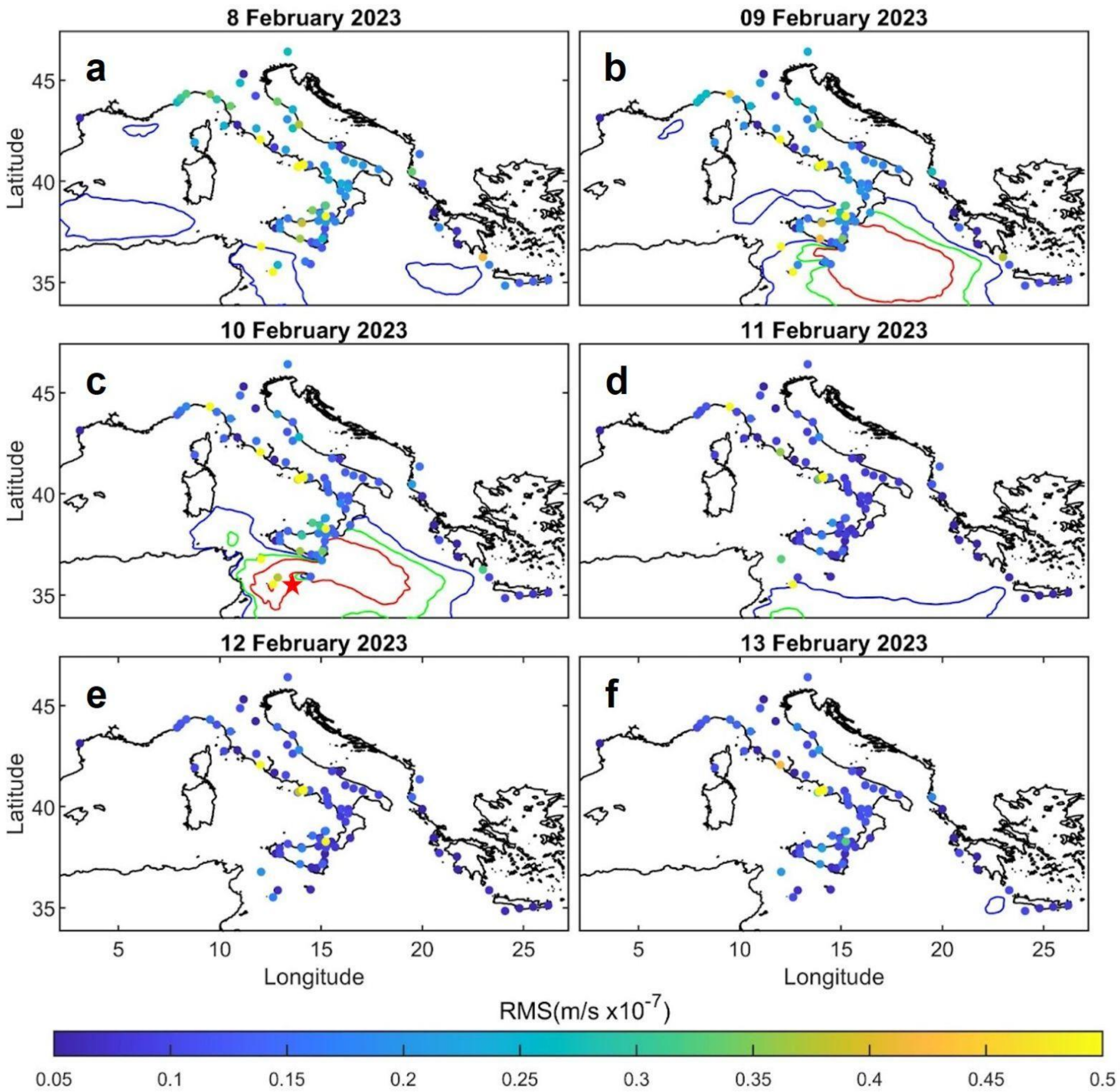

Figure S3: Spatial and temporal distribution of the RMS amplitude for the PM band computed at 105 stations considered (dots). The colors of dots represent the RMS amplitude as specified in the color bar. The blue, green and red contour lines represent significant wave heights of 3, 4 and 5 m, respectively, while the red five-point star in (c) indicates the eye position of the sub-tropical system Helios obtained from satellite images.

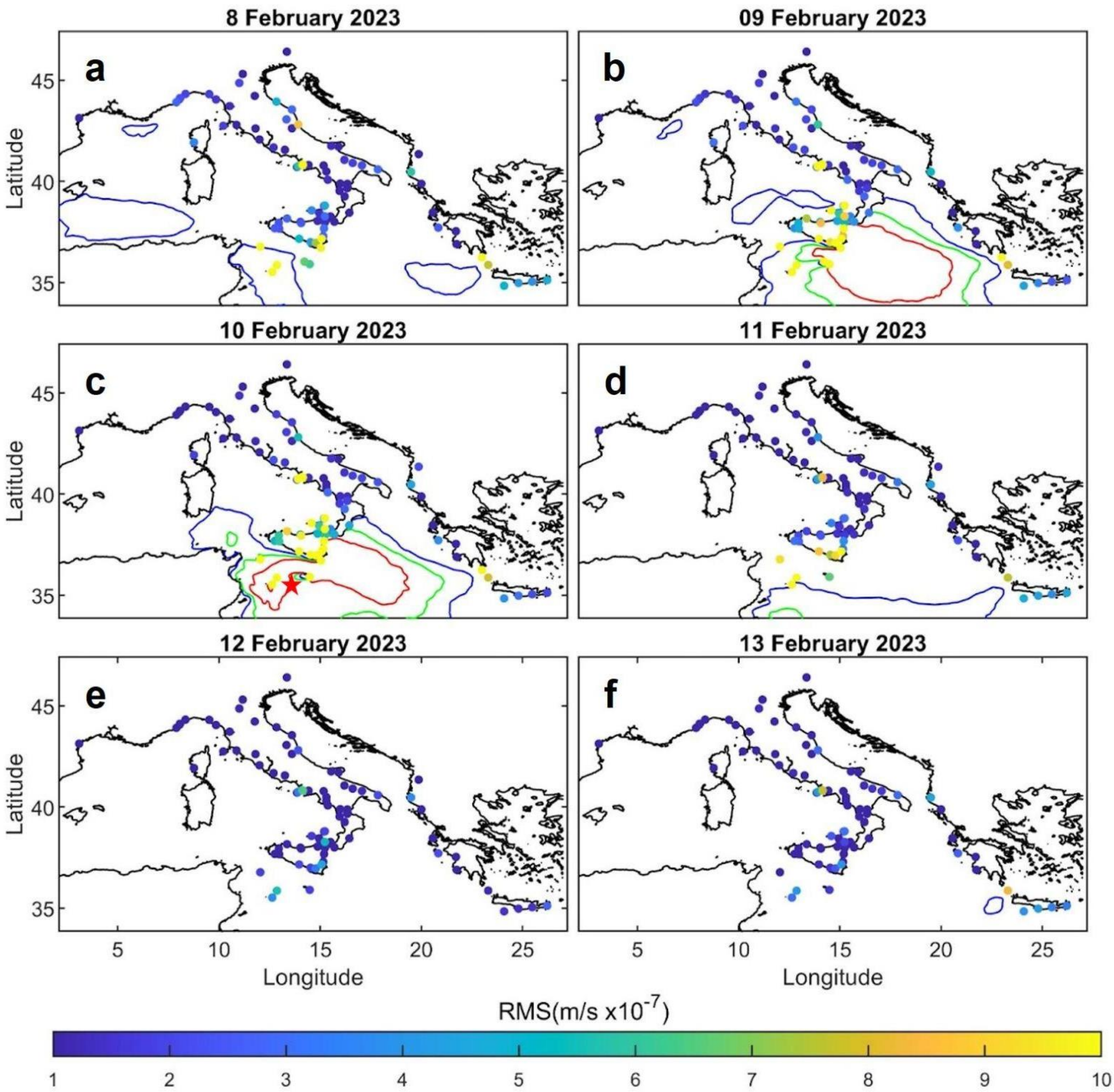

Figure S4: Spatial and temporal distribution of the RMS amplitude for the SPSM band computed at 105 stations considered (dots). The colors of dots represent the RMS amplitude as specified in the color bar. The blue, green and red contour lines represent significant wave heights of 3, 4 and 5 m, respectively, while the red five-point star in (c) indicates the eye position of the sub-tropical system Helios obtained from satellite images.

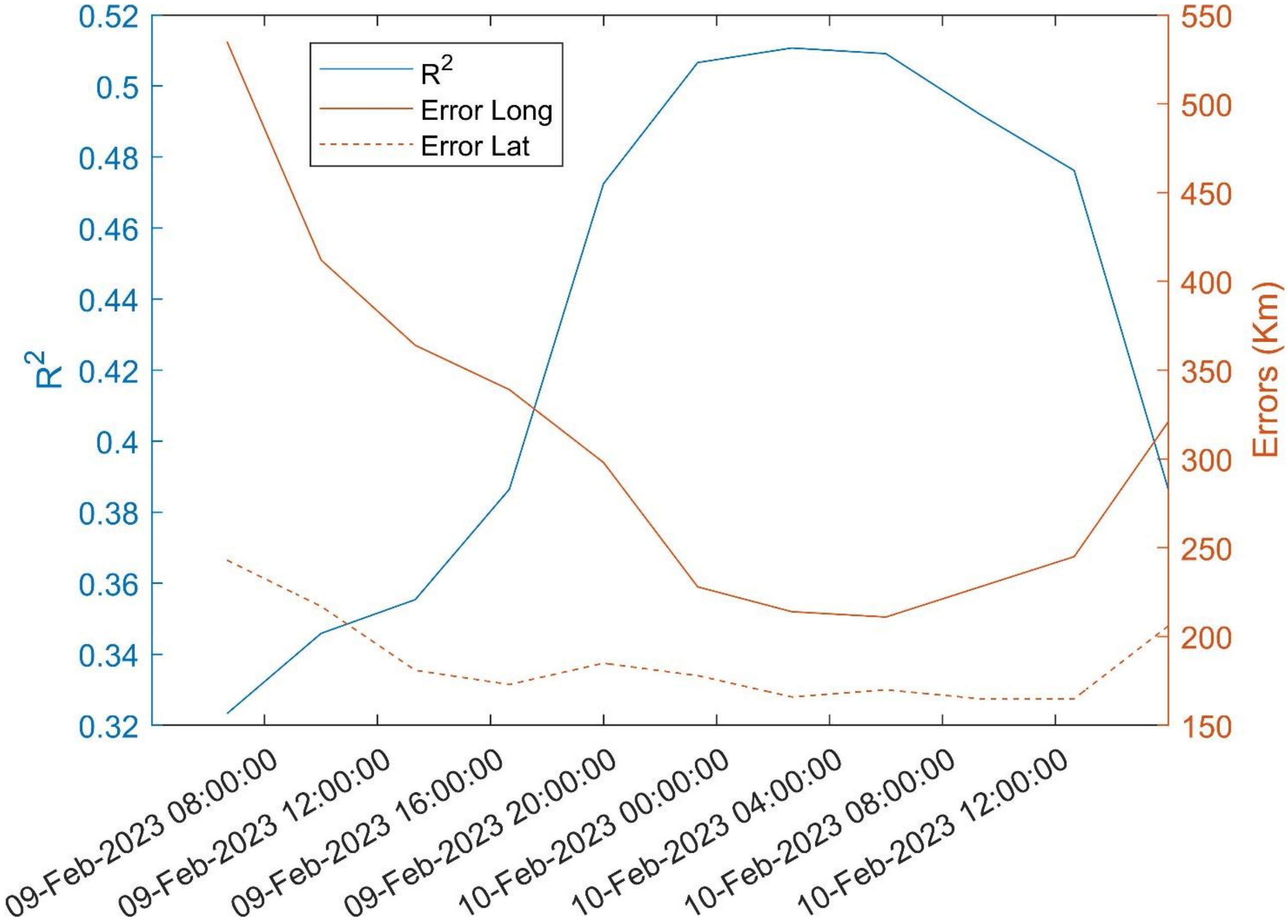

Figure S5: Plot showing the inversely proportional relationship between the errors (orange lines) and the R^2 (blue line).

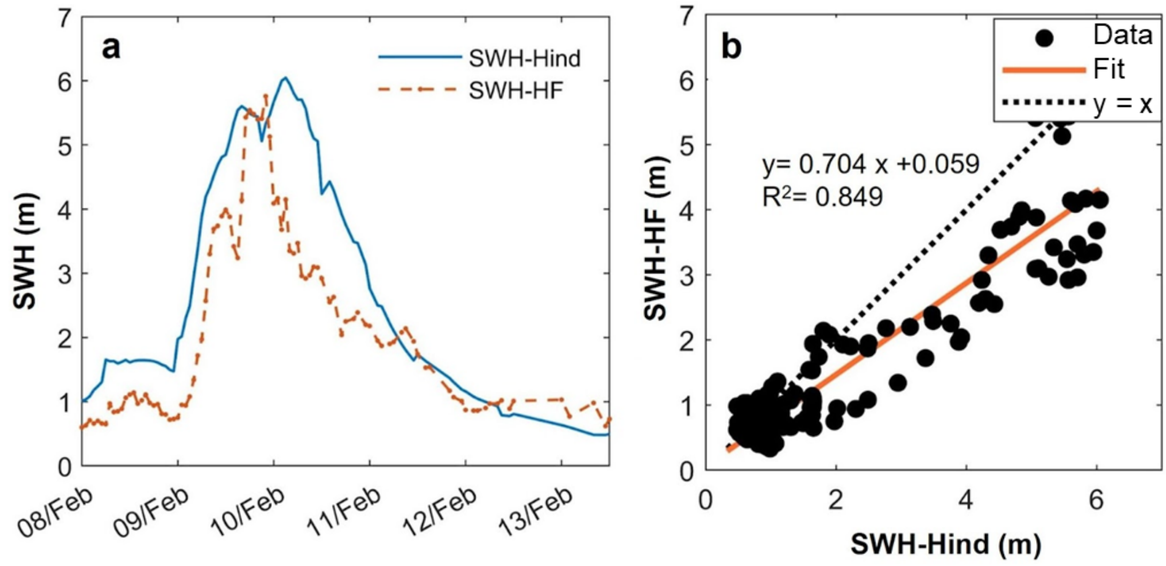

Figure S6: (a) Comparison between the SWH time series retrieved from hindcast data (SWH-Hind; light-blue line) and from HF Radar data (SWH-HF; orange dashed line). (b) Crossplot showing the agreement between SWH-Hind and SWH-HF data with a R^2 of 0.849. For the HF Radar location see **Figure 2c.**

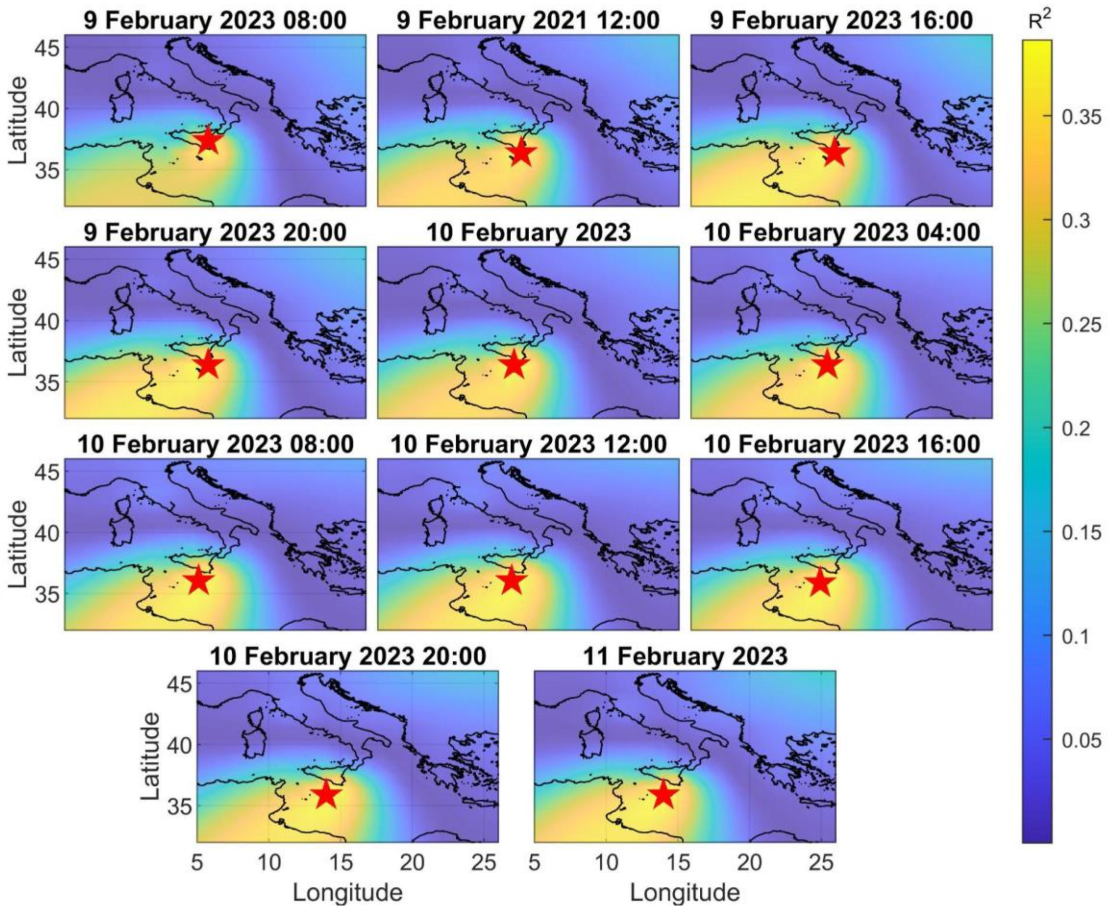

Figure S7: Spatial distribution of R^2 values during the entire period when we obtained reliable locations. The red five-point star indicates the centroid position of all the grid nodes whose R^2 values do not differ by more than 1% from the maximum R^2 value.

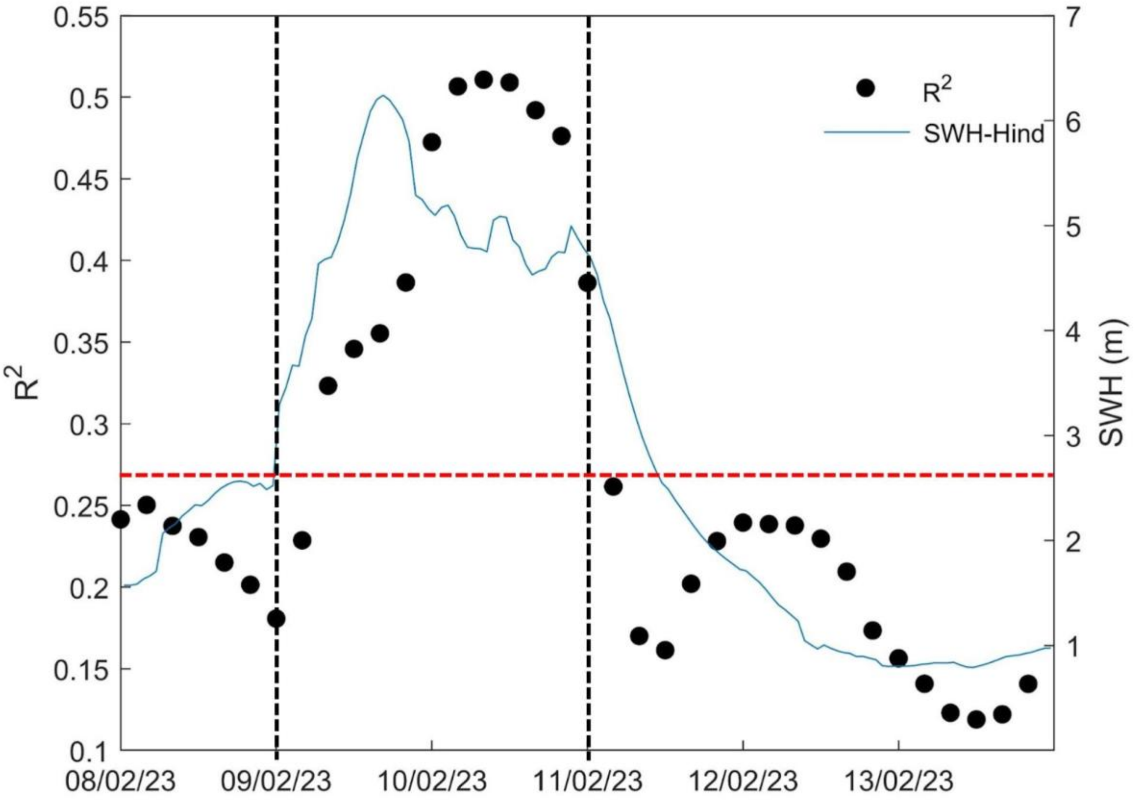

Figure S8: Scatter plot showing the time series of the maximum R^2, obtained by the location analysis, and of the SWH-Hind, obtained by computing the median value of the SWH data within the area in **Figure 8d** . The black dashed lines represent the time interval when Helios reached its highest intensity while the red dashed line indicates the R^2 reliable threshold.

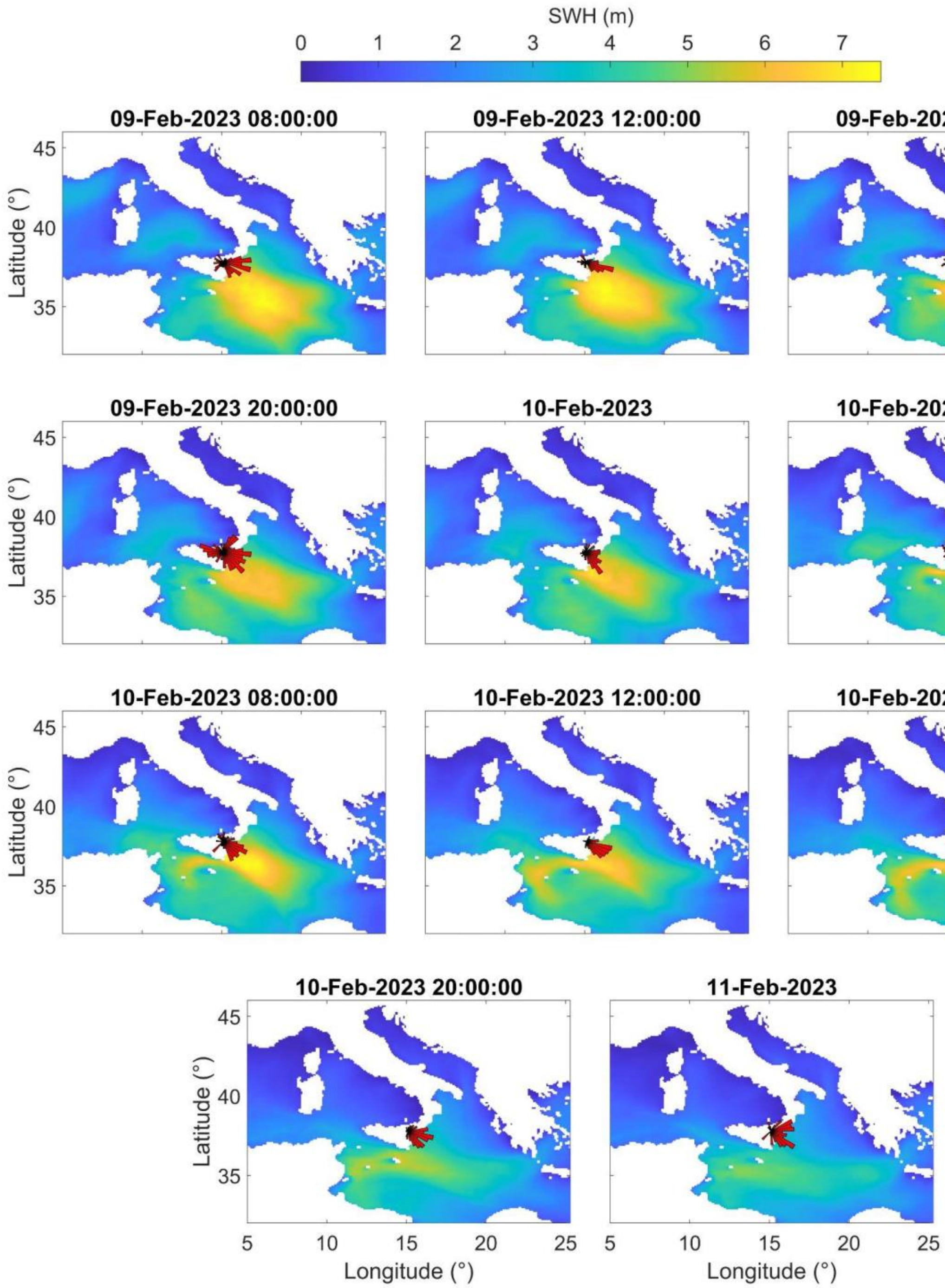

Figure S9: Hindcast maps showing the significant wave heights (in m) during the entire period when we obtained reliable locations by the grid search method. The rose diagram, located at the center of the Etna seismic permanent network (see **Figure 2b**), shows the distribution of the back azimuth values computed by the f–k analysis for the PM frequency band.

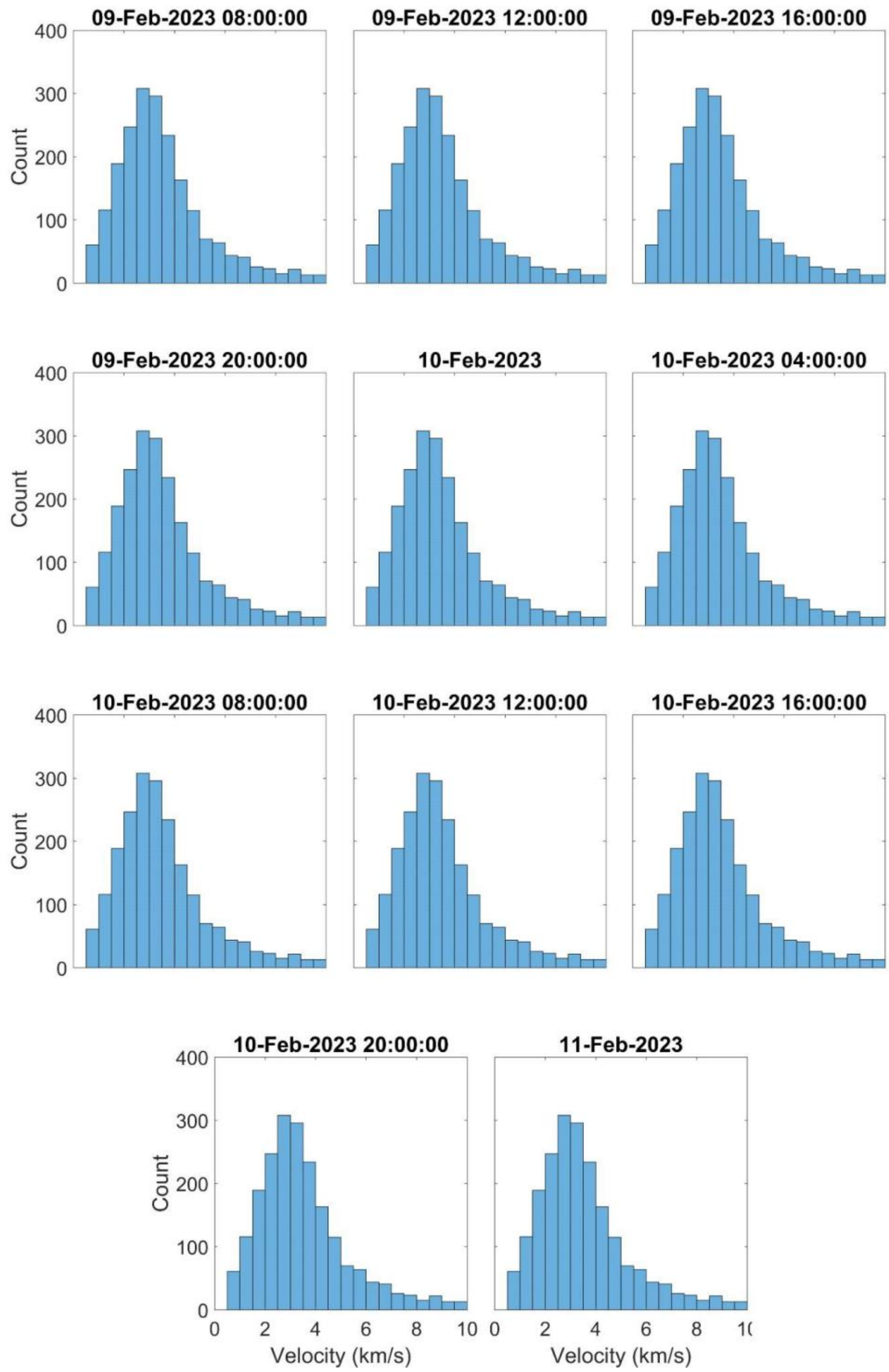

Figure S10: Distribution of apparent velocity values computed by f-k analysis for the PM frequency band. These values were calculated during the entire period when we obtained reliable locations by the grid search method.

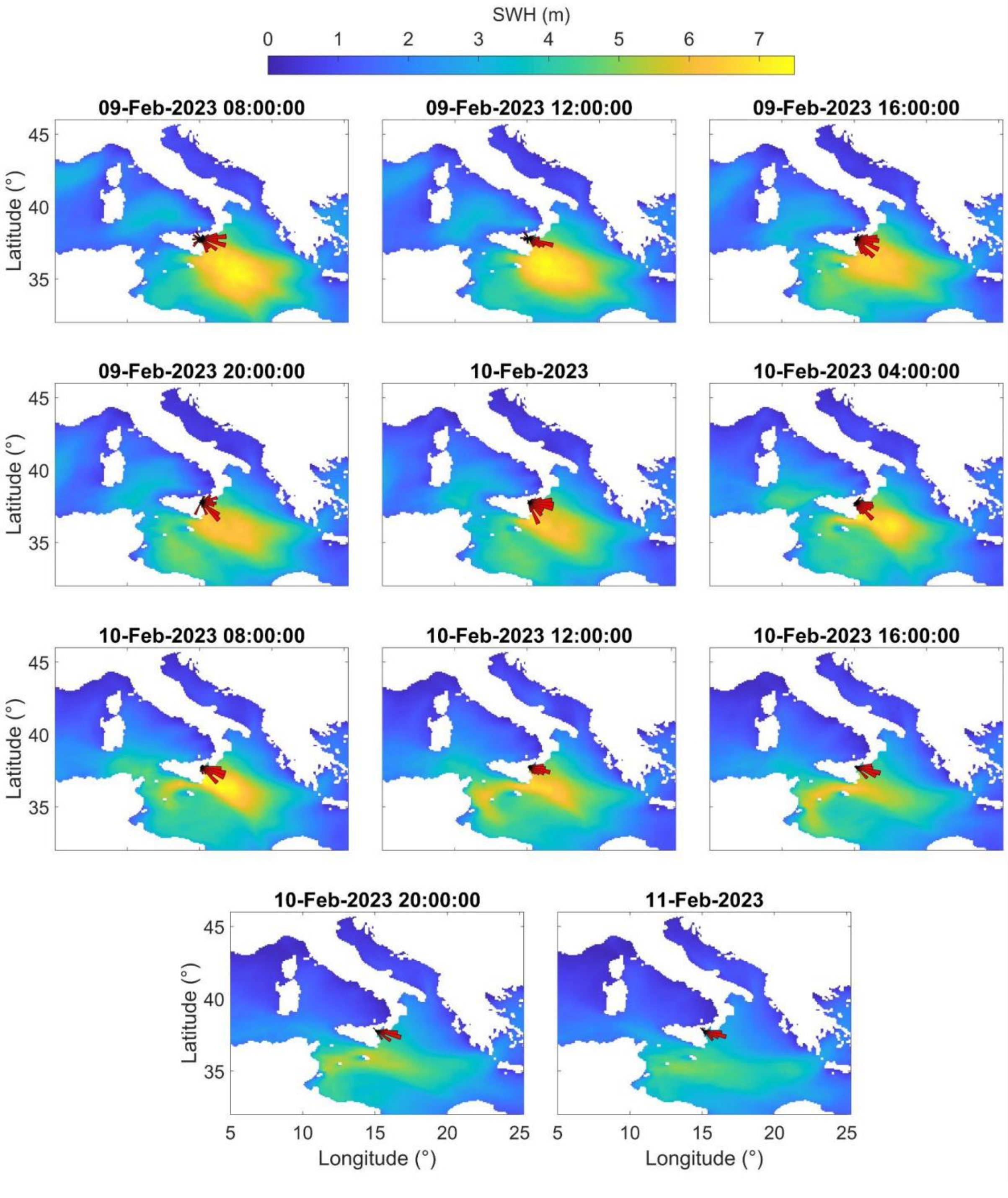

Figure S11: Hindcast maps showing the significant wave heights (in m) during the entire period when we obtained reliable locations by the grid search method. The rose diagram, located at the center of the Etna seismic permanent network (see **Figure 2b**), shows the distribution of the back azimuth values computed by f–k analysis for the SM frequency band.

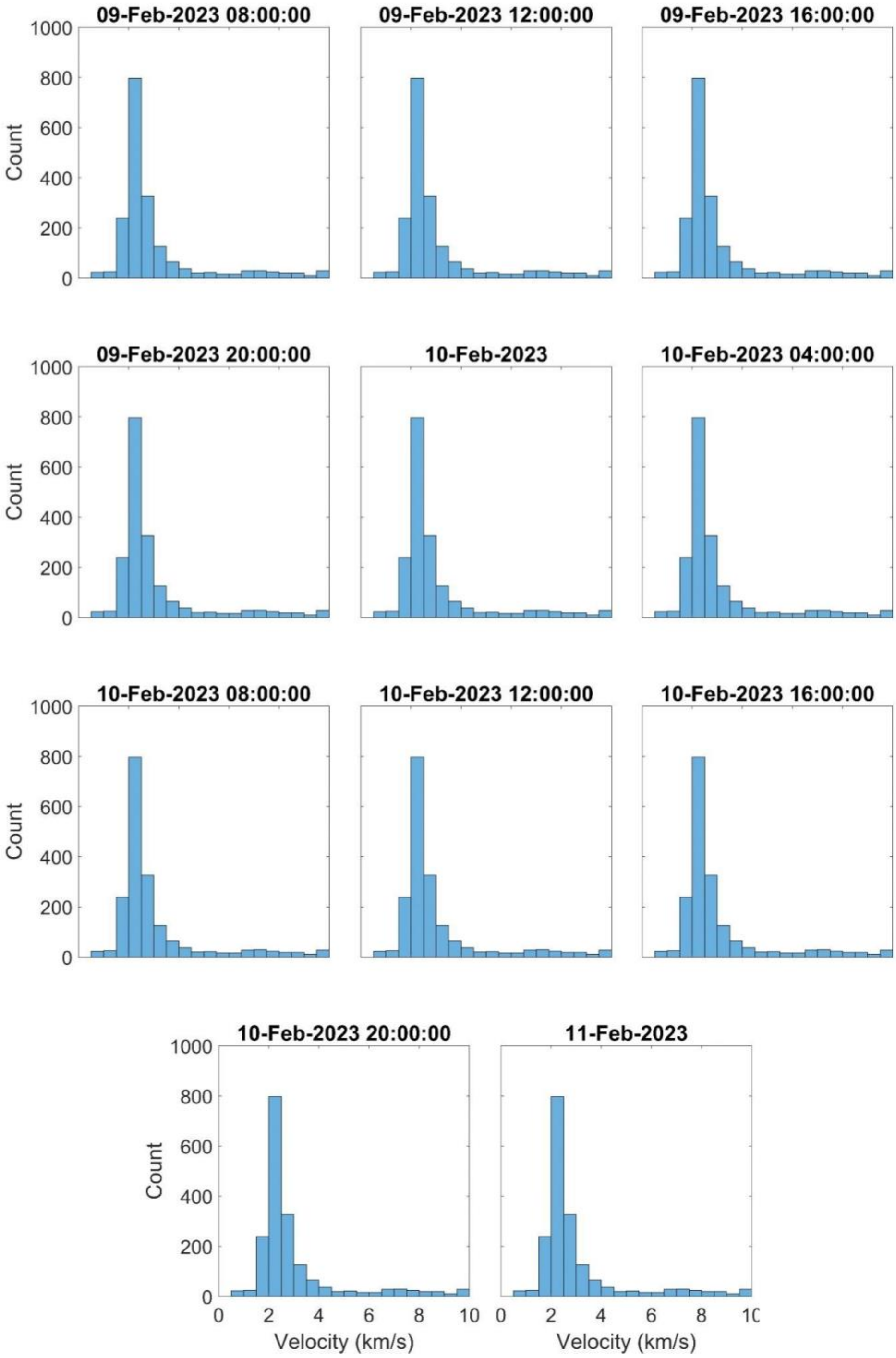

Figure S12: Distribution of apparent velocity values computed by f-k analysis for the SM frequency band. These values were calculated during the entire period when we obtained reliable locations by the grid search method.

Supplementary Tables

N	Name	Latitude (degrees)	Longitude (degrees)	Altitude (m a.s.l.)	Sensor	Network
1	QLNO	44.32	8.34	547	NANOMETRICS TRILLIUM-40S	IV
2	MSSA	44.31	9.51	93	NANOMETRICS TRILLIUM-40S	IV
3	PLMA	44.05	9.85	22	NANOMETRICS TRILLIUM-240S	IV
4	CELB	42.74	10.21	742	NANOMETRICS TRILLIUM-40S	IV
5	CASP	42.79	10.86	390	NANOMETRICS TRILLIUM-40S	IV
6	LATE	42.61	11.80	610	NANOMETRICS TRILLIUM-40S	IV
7	TOLF	42.06	12.00	371	NANOMETRICS TRILLIUM-40S	IV
8	LAV9	41.68	12.69	300	NANOMETRICS TRILLIUM-40S	IV
9	GIUL	41.56	13.25	566	NANOMETRICS TRILLIUM-40S	IV
10	MODR	41.14	13.87	345	NANOMETRICS TRILLIUM-40S	IV
11	IFOR	40.71	13.85	170	GURALP CMG-40T-60S	IV
12	IMTC	40.72	13.87	59	GURALP CMG-40T-60S	IV
13	IOCA	40.74	13.90	123	GURALP CMG-40T-60S	IV
14	CFMN	40.83	14.09	59	GURALP CMG-3ESPC-120S	IV

15	CPOZ	40.82	14.11	2	GURALP CMG-40T-60S	IV
16	COLB	40.82	14.14	22	GURALP CMG-40T-60S	IV
17	VTIR	40.80	14.42	612	GURALP CMG-40T-60S	IV
18	MCRV	40.78	15.16	1191	NANOMETRICS TRILLIUM-40S	IV
19	CDRU	40.49	15.30	1057	NANOMETRICS TRILLIUM-40S	IV
20	CMPR	40.32	15.30	732	NANOMETRICS TRILLIUM-40S	IV
21	BULG	40.08	15.37	815	NANOMETRICS TRILLIUM-40S	IV
22	CET2	39.53	15.95	675	NANOMETRICS TRILLIUM-40S	IV
23	CAR1	39.25	16.21	680	NANOMETRICS TRILLIUM-40S	IV
24	JOPP	38.60	15.88	500	NANOMETRICS TRILLIUM-40S	IV
25	MTTG	38.00	15.69	484	NANOMETRICS TRILLIUM-40S	IV
26	IST3	38.79	15.23	255	NANOMETRICS TRILLIUM-40S	IV
27	ISTR	38.78	15.19	103	NANOMETRICS TRILLIUM-40S	IV
28	IACL	38.53	14.35	145	NANOMETRICS TRILLIUM-40S	IV
29	IFIL	38.56	14.57	277	NANOMETRICS TRILLIUM-40S	IV
30	ILOS	38.44	14.94	283	NANOMETRICS TRILLIUM-40S	IV
31	IVPL	38.37	14.98	486	NANOMETRICS TRILLIUM-40S	IV
32	PII	43.72	10.52	66	NANOMETRICS TRILLIUM-120S	IV
33	MMN	39.89	15.99	921	NANOMETRICS	IV

					TRILLIUM-40S	
34	TDS	39.66	16.33	244	NANOMETRICS TRILLIUM-120C	IV
35	DGI	40.31	9.606	354	NANOMETRICS TRILLIUM-40S	IV
36	SSY	37.15	15.07	600	NANOMETRICS TRILLIUM-40S	IV
37	MPG	38.16	13.36	600	LENNARTZ LE3D-20S	IV
38	GIB	37.99	14.02	1020	NANOMETRICS TRILLIUM-120S	IV
39	PLAC	38.44	16.43	602	NANOMETRICS TRILLIUM-40S	IV
40	SALB	39.87	16.34	1000	NANOMETRICS TRILLIUM-40S	IV
41	MESG	40.58	17.85	78	NANOMETRICS TRILLIUM-40S	IV
42	NOCI	40.78	17.06	420	NANOMETRICS TRILLIUM-40S	IV
43	AMUR	40.90	16.60	443	NANOMETRICS TRILLIUM-40S	IV
44	MRVN	41.06	16.19	610	NANOMETRICS TRILLIUM-40S	IV
45	CAPA	41.15	15.81	156	NANOMETRICS TRILLIUM-120C	IV
46	MSAG	41.71	15.90	890	NANOMETRICS TRILLIUM-40S	IV
47	APRC	41.75	15.54	672	NANOMETRICS TRILLIUM-120C	IV
48	FRES	41.97	14.66	414	NANOMETRICS TRILLIUM-40S	IV
49	TERO	42.62	13.60	673	NANOMETRICS TRILLIUM-40S	IV
50	TRTR	42.80	13.91	160	NANOMETRICS TRILLIUM-40S	IV
51	GUMA	43.06	13.33	574	NANOMETRICS TRILLIUM-120S	IV

52	AOI	43.55	13.60	530	NANOMETRICS TRILLIUM-40S	IV
53	PESA	43.94	12.84	221	NANOMETRICS TRILLIUM-40S	IV
54	BRIS	44.22	11.76	260	NANOMETRICS TRILLIUM-120S	IV
55	CAVE	44.86	11.00	18	NANOMETRICS TRILLIUM-120S	IV
56	TEOL	45.36	11.67	370	NANOMETRICS TRILLIUM-120S	IV
57	STAL	46.26	12.71	625	NANOMETRICS TRILLIUM-120S	IV
58	OPPE	45.30	11.17	20	NANOMETRICS TRILLIUM-40S	IV
59	PTCC	46.40	13.35	700	NANOMETRICS TRILLIUM-40S	IV
60	AGLI	41.12	9.173	180	NANOMETRICS TRILLIUM-40S	IV
61	CAVT	37.67	12.75	158	GURALP CMG-3EX	IV
62	MMGO	37.66	12.97	397	NANOMETRICS TRILLIUM-120C	IV
63	CLTA	37.15	13.96	246	NANOMETRICS TRILLIUM-40S	IV
64	HPAC	36.70	15.03	70	NANOMETRICS TRILLIUM-40S	IV
65	HAGA	37.28	15.15	126	NANOMETRICS TRILLIUM-40S	IV
66	EPOZ	37.67	15.18	124	GURALP CMG-3EX	IV
67	MBFT	37.94	12.95	520	NANOMETRICS TRILLIUM-120S	IV
68	CSLB	37.93	14.05	583	NANOMETRICS TRILLIUM-120S	IV
69	MUCR	38.04	14.87	1042	NANOMETRICS TRILLIUM-40S	IV
70	MILZ	38.27	15.23	0	NANOMETRICS	IV

					TRILLIUM-40S	
71	MPNC	38.14	15.35	479	NANOMETRICS TRILLIUM-40S	IV
72	MSRU	38.26	15.50	408	NANOMETRICS TRILLIUM-40S	IV
73	AIO	37.97	15.23	751	NANOMETRICS TRILLIUM-40S	IV
74	IMI	43.91	7.893	840	NANOMETRICS TRILLIUM-40S	IV
75	RORO	44.11	8.066	246	NANOMETRICS TRILLIUM-40S	IV
76	AJAC	41.93	8.76	27	CMG3-ESPC broad band triaxial sensor by Guralp	FR
77	CLAF	43.13	3.09	115	CMG3-ESP broad band triaxial sensor by Guralp	FR
78	PYL	36.89	21.74	226	Trillium 40, 40 s, 1553 V/m/s-Trident, 16 vpp	HP
79	AMT	37.53	21.70	482	Trillium 40, 40 s, 1553 V/m/s-Trident, 16 vpp	HP
80	KNDR	35.23	23.62	13	CMG-3ESP, 120 s, 2000 V/m/s-RT130	HC
81	LTHK	37.70	20.83	35	CMG-3T, 120 s, 1500 V/m/s-Trident, 40 Vpp	HP
82	KTHA	36.25	23.06	360	STS-2, 120 s, 1500 V/m/s, generation 3 electronics	HL
83	VLO	40.46	19.49	80	NANOMETRICS TRILLIUM-40S	AC
84	PZIN	36.81	11.97	205	NANOMETRICS TRILLIUM-40S	IV
85	LPDG	35.51	12.63	50	NANOMETRICS TRILLIUM-40S	IV
86	ANKY	35.86	23.30	143	CMG-3ESP, 60 s,	HL

					2000 V/m/s-PS6-24	
87	KTHR	36.24	22.99	270	CMG-3ESP, 120 s, 2000 V/m/s-DM-24 Mk3	HC
88	GVD	34.83	24.08	170	STS-2, 120 s, 1500 V/m/s	HL
89	PFKS	35.04	25.47	745	CMG-3ESP, 120 s, 2000 V/m/s-RT130	HC
90	TIR	41.34	19.86	247	STRECKEISEN STS-1H-VBB	MN
91	FSK	38.45	20.56	113	CMG-3T, 120 s, 1500 V/m/s-DM-24 Mk2	HP
92	IMOD	34.97	24.79	243	CMG-3ESP, 120 s, 2000 V/m/s-RT130	HC
93	ZKR	35.11	26.21	254	STS-2, 120 s, 1500 V/m/s	HL
94	PGHD	36.77	12.04	331	NANOMETRICS TRILLIUM-40S	IV
95	HMDC	36.96	14.78	600	NANOMETRICS TRILLIUM-40S	IV
96	HVIT	36.99	14.52	296	GURALP CMG-3EX	IV
97	SRN	39.88	20.00	20	NANOMETRICS TRILLIUM-40S	AC
99	WDD	35.83	14.52	15	STRECKEISEN STS-2-120S	MN
100	LINA	35.86	12.86	70	NANOMETRICS TRILLIUM-40S	IV
101	MSDA	35.90	14.48	48	NANOMETRICS TRILLIUM-120S	ML
102	XLND	36.03	14.22	6	NANOMETRICS TRILLIUM-120S	ML
103	IWAV5	36.72	14.83	18	CERTIMUS - GURALP	
104	IWAV3	36.87	14.44	47	CERTIMUS - GURALP	

105	IWAV2	36.92	14.68	607	CERTIMUS - GURALP	

Table S1. List of stations used for the spectral analysis and in the grid search method and their features in terms of locations and sensor type.

N	Name	Longitude (degrees)	Latitude (degrees)	Altitude (m a.s.l.)	Sensor
1	EPLC	14.9857	37.7651	2917	Nanometrics Trillium 40S
2	ESVO	14.9469	37.7731	1691	Nanometrics Trillium 40S
3	ESPC	15.0274	37.6925	1610	Nanometrics Trillium 40S
4	ESLN	14.9744	37.6934	1735	Nanometrics Trillium 40S
5	EPIT	15.0567	37.8113	1586	Nanometrics Trillium 40S

6	EPDN	15.0168	37.7659	2823	Nanometrics Trillium 40S
7	EMPL	14.9703	37.6790	1438	Nanometrics Trillium 40S
8	EMFO	15.0902	37.7357	1163	Nanometrics Trillium 40S
9	ECZM	14.9041	37.7313	1346	Nanometrics Trillium 40S
10	ECPN	14.9865	37.7437	2996	Nanometrics Trillium 40S
11	ECNE	15.0018	37.7653	2901	Nanometrics Trillium 40S
12	ECBD	15.0865	37.7802	1419	Nanometrics Trillium 40S
13	EMNR	15.0260	37.8168	1797	Nanometrics Trillium 40S
14	EMSG	14.9495	37.8215	1435	Nanometrics Trillium 40S
15	EMFS	14.9979	37.7196	2507	Nanometrics Trillium 40S

Table S2. List of stations used in the array method and their features in terms of locations and sensor type.